Effects of impurity scattering and transport topology on exciton migration and trapping: An experimental study of quasi-one-dimensional molecular crystals

D. D. Dlott, M. D. Fayer,[a] and R. D. Wieting

Department of Chemistry, Stanford University, Stanford, California 94305
(Received 25 May 1978)

A series of experiments in which the time resolved triplet x-trap emission from single crystals of 1,2,4,5-tetrachlorobenzene (TCB) at 1.35°K is presented for various concentrations of the doped-in scattering impurity, d_2-TCB. It is demonstrated that exciton-impurity scattering is the dominant process affecting macroscopic exciton transport and trapping. The time-dependent trapping rate is found to be proportional to the inverse square root of the scattering impurity concentration in agreement with theoretical prediction. This implies that transport is close to strictly one-dimensional. Excellent agreement between the data and a model involving microscopically incoherent transport is found, but the data also shows generally good agreement with a model employing microscopically coherent transport. From the concentration dependence and time-dependent trapping curves, an upper bound of $\sim 5 \times 10^3$ sec^{-1} can be placed on the frequency of multidimensional steps between one-dimensional chains. Transport is macroscopically diffusive. The basic parameters characterizing long range exciton migration and trapping are obtained.

I. INTRODUCTION

The transport of Frenkel excitons[1] in molecular crystals has been examined by a wide variety of experimental and theoretical methods for a considerable number of years and yet basic questions concerning the fundamental processes which govern exciton transport remain unanswered. It is clear that the strengths of intermolecular interactions,[2] the extent of exciton-phonon[3,4a] and exciton-impurity scattering,[4b,5-7] the rate of exciton trapping[2c,6-9] and the topology of exciton transport[7] all influence the overall nature of exciton migration. Experimental techniques which have been employed as probes of transport include optical absorption and lineshape analysis,[4,5,10] optically detected magnetic resonance,[2a] spin-locking experiments,[11] spin-echo measurements[2d] and the observation of trap optical emission in both steady state[2c,8a] and time-resolved[4,12,13] experiments. In this paper we will focus our attention on the time dependence of trap optical emission following impulse excitation of the host exciton band since this experimental observable can be related to the macroscopic dynamics of exciton transport and it is strongly influenced by the processes mentioned above. In a recent theoretical study, a detailed model of the effect of impurity scattering on the time-dependence of trapping of excitons undergoing basically one-dimensional transport was presented.[7] Both the coherent (wavelike) and incoherent (diffusive) microscopic modes of transport were considered and the effects of deviations from strictly one-dimensional transport topology (quasi-one-dimensional) were treated in detail. In one dimensional systems well-defined impurity scattering sites,[14] i.e., impurities having excited states with higher energy than the corresponding host molecule excited state and which are not amalgamated[4b] into the host exciton band, can severely inhibit transport by "caging" a mobile exciton.[6,7] That is, the exciton is restricted to a chain of molecules bounded by scattering sites until it either tunnels past a scattering site at one of the ends or takes a non-one-dimensional step to an adjacent linear chain. Exciton trapping in this type of system is governed by a time-dependent trapping rate function which has a form dependent on the microscopic mode of transport, the topology of transport and various physical parameters of the system. Only in the case of nearly isotropic transport does this time-dependent trapping rate function reduce to a time-independent trapping rate constant.

Several recent experimental studies[13] of exciton trapping in one-dimensional systems have employed phenomenological trapping *rate constants* and rate equations which neglect the effects of scattering impurities and deviations from a strictly one-dimensional transport topology. This led to incomplete interpretations of observed results. Although not nearly as visible as their trap counterparts, scattering impurities can play the dominant role in exciton transport and in trapping experiments in one-dimensional systems by forcing the macroscopic mode of transport to be diffusive regardless of the microscopic transport mode.[6,7] The influence of scattering impurities on observables associated with trapping in one-dimensional systems was suggested in a preliminary study on time dependent trap emission in the 1, 2, 4, 5-tetrachlorobenzene triplet exciton system.[6] In that experiment, the time-dependent optical emission from the x-trap found in neat crystals of TCB was shown to be explicable in terms of the effects of impurity scattering on exciton transport. The scattering impurity was taken to be the naturally occurring isotopic impurity of mondeutero TCB. Thus, even in so called "pure crystals," intrinsic scattering species, which may be isotopic impurities, lattice defects, or difficult to remove chemical impurities, cannot be neglected. It has long been recognized that traps are present even in the most highly purified samples of molecular crystals. This is demonstrated by the fact that there is some degree of trap optical emission at very low temperatures from virtually all crystals. It is much

[a]Alfred P. Sloan Fellow.

 0021-9606/78/6906-2752$01.00

more difficult to directly detect impurities with excited state energies above that of the host crystal's exciton band since these exciton scattering species do not undergo activated luminescence and their low concentration makes detection in an absorption experiment all but impossible.

In this paper a series of experiments is presented which demonstrate the applicability of the recently published model of exciton migration, impurity scattering, and trapping in one-dimensional systems. These experiments measure the time-dependence of optical emission from the triplet x-trap found in crystals of 1, 2, 4, 5-tetrachlorobenzene (TCB) following impulse excitation of the TCB triplet exciton bands. A series of samples containing a range of known concentrations of the isotopic scattering impurity d_2-TCB is employed, and the results compared to the predictions of the model. Excellent overall agreement is shown between theory and experiment. The observed trapping rate was found to be proportional to the inverse square root of scattering impurity mole fraction. This concentration dependence is in exact agreement with theoretical prediction, [7] and demonstrates that impurity scattering determines the rate of exciton trapping in the TCB systems studied. From the observed concentration dependence and the physical parameters associated with the TCB system, it is possible to place an upper limit of 10^5 sec^{-1} on the frequency of cross-chain steps in this system.

Detailed analysis of the experimental time dependent trapping curves provides a better estimate of the cross chain stepping frequency. If exciton transport in TCB is strictly one-dimensional then a model assuming microscopically *incoherent* transport is found to be consistent with the observed trapping results when the formalism of Knox and Kenkre[3a] is used to calculate the one-dimensional site-to-site hopping frequency. In terms of the strength of the cross-chain intermolecular interactions, the definition of strictly one-dimensional varies with the physical parameters of the particular molecular crystal. A system is strictly one-dimensional if the probability of taking a cross-chain step is vanishingly small during a time period corresponding to the exciton excited state lifetime. Strictly one-dimensional calculations for microscopically coherent transport give results which are somewhat too slow to account for the experimental data. However, a cross chain stepping frequency of less than 5×10^3 sec^{-1} produces an increase in the rate of trapping sufficiently great to bring calculations using a coherent quasi-one-dimensional transport model into agreement with observation. Therefore a better estimate of the cross chain stepping frequency is $<5\times10^3$ sec^{-1}.

The net result is that independent of the microscopic mode of transport, impurity scattering forces exciton transport in quasi-one-dimensional systems to be macroscopically diffusive. Macroscopic transport is characterized by the exciton cage-to-cage stepping frequencies which are obtained from the analysis of the trapping concentration dependence and the time-dependent trapping curves.

II. THE TRAPPING EQUATIONS

Well-defined scattering sites have a transport blocking effect which causes an exciton to remain confined to a linear chain of molecules between two such sites, a cage, for a relatively long time before tunneling past an impurity site onto an adjacent chain of molecules. During this time the exciton probability will become uniformly distributed in the initial cage, ensuring equal probability of a step to either adjacent cage. Thus, the transport will describe a random walk between cages on the infinite linear chain when viewed on a time scale long relative to the time required to tunnel out of a particular cage. Such transport is strictly one-dimensional. [6,7]

A more complete treatment of one-dimensional systems includes the effects of very small interactions leading to transport between adjacent linear chains. [7] This motion will be incoherent in nature since local potential fluctuations will certainly be much larger than cross chain interactions in systems near the one-dimensional limit. The frequencies of interchain steps will be quite small compared to the frequency of site-to-site motion along a given linear chain. However, an interchain step is a step to a different cage, while on chain a great number of site-to-site steps occur before enough encounters with the caging scattering impurities permit a single cage step. Thus, the frequency of steps between cages on adjacent chains may be comparable to or greater than the frequency of steps between cages on a single chain. This results in a change in the effective exciton transport topology. Transport will be a two- or three-dimensional random walk (not necessarily isotropic) between linear cages, supersites, on the superlattice, i.e., the lattice of all linear cages. This will have a significant effect on trapping since multidimensional random walks greatly increase the total number of distinct lattice sites sampled[15] with a concomitant increase in the probability that an exciton will sample a low concentration trap site.

The caging effect of well-defined scattering impurities also has an important consequence for the trapping event. An exciton in such a system is confined to a small set of molecules in a cage for a relatively long time, so that if a trap site is present in that cage the exciton-trap interaction time is greatly extended and the exciton will trap on its first visit to the cage, even if the single encounter trapping probability is quite small. [6,7]

The model presented below is the result of the above considerations applied to the time evolution of an exciton population ensemble interacting with dilute scattering and trapping impurities in a one-dimensional system. [7] The time-dependent populations of the band states $E(t)$ and the trap states $T(t)$ are described by the rate equations

$$\dot{E}(t) = -[K_E + K_L(t)]E(t) \tag{1a}$$

$$\dot{T}(t) = -K_T T(t) + K_L(t)E(t). \tag{1b}$$

K_E is the decay rate constant (inverse lifetime) for band states and K_T is the decay rate constant for trap states.

Thermally assisted promotion from a localized trap state is not included in this scheme, since it is negligible at sufficiently low temperatures.[11] $K_L(t)$ is the instantaneous rate of exciton localization per unit population, the *time-dependent trapping rate function*, the form of which depends on the effective transport topology. For impulse duration excitation of the system, the solutions in Eq. (1) require only the form of $K_L(t)$. In what follows, N_T is the trap concentration, χ is the scattering impurity concentration, β is the intermolecular interaction matrix element responsible for on chain one-dimensional transport, and S is the energy difference between the scattering impurity site excited state energy and the exciton band center.

A. Strictly one-dimensional transport

The time-dependent trapping rate function for strictly one-dimensional systems is given by

$$K_L(t) = At^{-1/2}, \tag{2}$$

and is independent of the microscopic mode of transport.[7] The value of the trapping rate coefficient, A, does depend on the mode of transport and can be evaluated using the parameters of the system, all of which are amenable to experimental determination.

For an ensemble of coherent excitons (exciton–photon scattering is slow relative to exciton-impurity scattering) at temperature T, the trapping coefficient is

$$A_{\mathrm{COH}} = \frac{2^{3/2}\Gamma(5/4)I_{3/4}(y)}{(y/2)^{3/4}I_0(y)} \times \frac{N_T\chi}{[\ln(1/1-\chi)]^{3/2}} \frac{|\beta|^{3/2}}{\hbar^{1/2}S} \tag{3}$$

where $y = |2\beta/KT|$ and I_0 and $I_{3/4}$ are modified Bessel functions. For incoherent excitons (fast exciton-phonon scattering) with an on chain site-to-site stepping frequency ν_{INC}, the trapping coefficient is given by

$$A_{\mathrm{INCOH}} = \frac{N_T|\beta|}{S}\left[\frac{2(\chi^{-1}-1)\nu_{\mathrm{INC}}}{\pi}\left(\frac{1-P_e}{P_e}\right)\ln\left(\frac{1+P_e}{1-P_e}\right)\right]^{1/2} \tag{4a}$$

$$A_{\mathrm{INCOH}} = \frac{4\pi\beta^2 N_T}{\hbar S}\left[\frac{2(\chi^{-1}-1)}{\alpha\pi}\left(\frac{1-P_e}{P_e}\right)\ln\left(\frac{1+P_e}{1-P_e}\right)\right]^{1/2} \tag{4b}$$

where Eq. (4b) has used the explicit form of ν_{INC} given by Knox and Kenkre,[3a]

$$\nu_{\mathrm{INC}} = \frac{16\pi^2\beta^2}{\alpha\hbar^2}. \tag{5}$$

The parameter α is the decay rate constant for the loss of coherence of the exciton state, and in principle can be determined from spectroscopic information (see Appendix II). The terms involving P_e in Eq. (4) correct for the probability of escape or "leakage" from the initial cage before a uniform distribution is achieved in that cage. If P_e becomes large, the results lose accuracy. In practice this somewhat limits the diluteness of impurities for which a calculation can be made. P_e is given by

$$P_e = 1 - \left(1 - \frac{2\beta^2}{S^2}\right)^{\langle n\rangle+1} \tag{6a}$$

$$\langle n\rangle = \left(\frac{2}{\pi}\right)^{1/2}(\chi^{-1}-1)\left[1 + \tfrac{3}{8}(\chi^{-1}-1)^{-2} - \tfrac{7}{128}(\chi^{-1}-1)^{-4} + \cdots\right], \tag{6b}$$

where $\langle n\rangle$ is the mean number of exciton collisions with the impurity site it last traversed before a uniform exciton probability distribution is achieved in the cage.[16]

Equations (3) and (4) show that the dependence of the rate of exciton trapping on scattering impurity concentration is basically identical for the coherent and incoherent microscopic modes of exciton transport. For coherent excitons, $A_{\mathrm{COH}} \propto \chi/[\ln(1/1-\chi)]^{3/2}$. However, for reasonably dilute impurities $\ln(1/1-\chi) = \chi$, so $A_{\mathrm{COH}} \propto \chi^{-1/2}$, which is also the dependence manifested by A_{INCOH}, Eq. (4), for incoherent excitons. Thus independent of the microscopic mode of transport, the concentration dependence can be used to access the transport topology and, as shown below, determine the frequency of cross chain steps. It is also worth noting that the rate of trapping varies relatively slowly with scattering impurity concentration.

Using Eqs. (1) to (6) the time-dependent exciton and trap populations are obtained for an exciton system which is strictly one-dimensional in its transport. A is obtained from Eq. (3) or (4).

$$E(t) = \exp[-K_E t - 2At^{1/2}] \tag{7a}$$

$$T(t) = \exp(-K_T t)\left(\frac{\pi A^2}{K_E - K_T}\right)^{1/2}\exp\left(\frac{A^2}{K_E - K_T}\right) \times\left[\operatorname{erf}\left([K_E - K_T)t]^{1/2} + \frac{A}{(K_E - K_T)^{1/2}}\right) - \operatorname{erf}\left(\frac{A}{(K_E - K_T)^{1/2}}\right)\right], \tag{7b}$$

where $\operatorname{erf}(x)$ is the error function of argument x.

B. Quasi-one-dimensional transport

For systems in which transport is close to but not strictly one-dimensional, an exciton undergoes a multidimensional random walk among the cages formed by the scattering impurities. Each cage, which is composed of many lattice sites, is a single supersite in the superlattice composed of all cages. An exciton performs a macroscopic random walk among the sites of the superlattice. This results in an identical time-dependent form of the trapping rate function for both microscopic modes of exciton migration,[7]

$$K_L(t) = K_L + B_L t^{-1/2}. \tag{8}$$

The values of the trapping parameters K_L and B_L depend on all of the physical parameters of the strictly one-dimensional problem and on the rate and relative anisotropy of the exciton walk on the three-dimensional superlattice.

The frequency of cage steps along the linear direction, denoted by ν_L, is given by the strictly one-dimensional

cage stepping frequency. For an ensemble of coherent excitons at temperature T, the thermal average frequency of cage steps is given by

$$\nu_L(\mathrm{COH}) = \frac{16\pi^{1/2}}{\chi^{-1}-1}\,\frac{|\beta|^3}{hs^2}\,\frac{I_{3/2}(y)}{(y/2)^{3/2}I_0(y)}\ , \tag{9}$$

where $y = |2\beta/KT|$ and I_0 and $I_{3/2}$ are modified Bessel functions. If the microscopic mode of transport is incoherent with a site-to-site stepping frequency ν_{INC}, the frequency of cage steps is given by

$$\nu_L(\mathrm{INCOH}) = \frac{\nu_{\mathrm{INC}}}{\chi^{-1}-1}\,\frac{\beta^2}{S^2}\left(\frac{1-P_e}{P_e}\right)\ln\left(\frac{1+P_e}{1-P_e}\right) \tag{10a}$$

or using Eq. (5),

$$\nu_L(\mathrm{INCOH}) = \frac{16\pi^2\beta^4}{(\chi^{-1}-1)\,\alpha h^2 S^2}\left(\frac{1-P_e}{P_e}\right)\ln\left(\frac{1+P_e}{1-P_e}\right)\ . \tag{10b}$$

Note that the dependence on χ, the scattering impurity mole fraction, is identical in Eq. (9) and Eq. (10) when P_e in Eq. (10) is small, i.e. when P_e is in its regime of usefulness.

Generalized three-dimensional arrangements of one-dimensional molecular chains employed in this model included cross chain motion through the use of two parameters, ν_C and $\nu_{C'}$, the frequencies of interchain steps in the two orthogonal off-chain directions. The relative probabilities for steps in different directions in the three-dimensional array of molecular chains are

$$\text{On chain:}\quad L = \nu_L/\nu_{\mathrm{TOT}}$$

$$\text{Interchain:}\begin{cases} C = \nu_C/\nu_{\mathrm{TOT}} \\ C' = \nu_{C'}/\nu_{\mathrm{TOT}} \end{cases}$$

$$\nu_{\mathrm{TOT}} = \nu_L + \nu_C + \nu_{C'}\ . \tag{11}$$

From these relative probabilities the two leading terms of the random walk Green's function can be obtained.[15] The remaining terms are negligible. The first term is the convergent integral

$$u_0 = \frac{1}{\pi^3}\int_0^{\pi}\!\!\int\!\!\int \frac{d\phi_1 d\phi_2 d\phi_3}{1-(L\cos\phi_1 + C\cos\phi_2 + C'\cos\phi_3)}\ . \tag{12}$$

In all cases this may be evaluated by numerical integration. However, if $\nu_C = \nu_{C'}$, i.e., $C = C'$, a convenient closed form expression is obtained,[17]

$$u_0 = \frac{1}{C}\,I([L/C]^{1/2}) \tag{13}$$

where $I(\alpha)$ is given by

$$I(\alpha) = 4[(\gamma+1)^{1/2} - (\gamma-1)^{1/2}]\,K(k_2)K(k_3)/\alpha\pi^2 \tag{14a}$$

$$k_2 = \tfrac{1}{2}[(\gamma-1)^{1/2} - (\gamma-3)^{1/2}][(\gamma+1)^{1/2} - (\gamma-1)^{1/2}] \tag{14b}$$

$$k_3 = \tfrac{1}{2}[(\gamma-1)^{1/2} + (\gamma-3)^{1/2}][(\gamma+1)^{1/2} - (\gamma-1)^{1/2}] \tag{14c}$$

$$\gamma = (4+3\alpha^2)/\alpha^2 \tag{14d}$$

and $K(k)$ is the complete elliptic integral of the first kind of modulus k. The second term is

$$u_1 = 1/(2\pi^2 LCC')^{1/2}\ . \tag{15}$$

The quasi-one-dimensional trapping rate parameters, K_L and B_L, are given by

$$K_L = N_T(\chi^{-1}-1)\,\frac{\nu_{\mathrm{TOT}}}{u_0} \tag{16}$$

$$B_L = \frac{N_T(\chi^{-1}-1)\,\nu_{\mathrm{TOT}}^{1/2}u_1}{\pi^{1/2}u_0^2}\ . \tag{17}$$

The concentration dependence of K_L and B_L contains information pertaining to the relative anisotropy of the random walk and hence about the magnitude of the interchain interactions. If $\nu_L \gg \nu_C$ and $\nu_{C'}$, then K_L and B_L are proportional to $(\chi^{-1}-1)^{1/2}$. This is essentially the one-dimensional behavior and indicates that such a system is very close to the strictly one-dimensional limit. However, if $\nu_L \approx \nu_C$ a stronger dependence on scattering impurity concentration results, and in the limit that $\nu_L \ll \nu_C$ and $\nu_{C'}$ the dependence goes as $(\chi^{-1}-1)$. The net effect can be to produce trapping which behaves topologically multidimensional even though the intermolecular interactions and the total extent of exciton motion is virtually one-dimensional.

The trapping rate parameters are used with Eq. (8) to solve the population rate equations, yielding the time-dependent populations

$$E(t) = \exp[-(K_E+K_L)\,t - 2B_L\,t^{1/2}] \tag{18a}$$

$$\begin{aligned} T(t) = \exp(-K_T t)\Bigg\{ & \frac{K_L}{K_L+K_E-K_T} \\ & \times\left(1-e^{-(K_L+K_E-K_T)t-2B_L t^{1/2}}\right) + \left(\frac{B_L^2\pi}{K_L+K_E-K_T}\right)^{1/2} \\ & \times e^{B_L^2/(K_L+K_E-K_T)}\left(1-\frac{K_L}{K_L+K_E-K_T}\right) \\ & \times\left[\mathrm{erf}\left([(K_L+K_E-K_T)t]^{1/2} + \frac{B_L}{(K_L+K_E-K_T)^{1/2}}\right)\right. \\ & \left.\left. - \mathrm{erf}\left(\frac{B_L}{(K_L+K_E-K_T)^{1/2}}\right)\right]\right\}\ , \end{aligned} \tag{18b}$$

where $\mathrm{erf}(x)$ is the error function of argument x. In the strictly one-dimensional limit, the expression of Eq. (7) should be used.

III. EXPERIMENTAL

TCB (Eastman Kodak) was three times recrystallized from ethanol, vacuum sublimed, and zone refined under N_2 for 200 passes. The center section of the zone-refined material was again zone-refined for 200 passes. Dideutero-TCB was synthesized from 99.5% C_6D_6 (Aldrich) by chlorination with Cl_2 gas. The d_2-TCB was recrystallized from ethanol, vacuum sublimed, and zone-refined. The concentration of d_2-TCB in each TCB sample was determined by quantitative preparation in the following way. Relatively high concentration samples were prepared by accurate weighing of the two materials followed by vacuum sublimation into individual crystal growing tubes. Single crystals were then grown from each mixture using the Bridgeman technique. Relatively low concentration samples were prepared in the same fashion by dilution of the more concentrated

samples. The temperature of the samples immersed in liquid He was monitored by measurement of the pressure of He vapor with a digital manometer. All the time-dependent trapping experiments were performed at 1.35 °K.

A $\frac{3}{4}$ meter Spex monochromator was used to characterize the phosphorescent x-trap and exciton spectra. In the time-resolved measurements, the initial triplet exciton population was prepared either by direct triplet excitation with a 20 nsec doubled ruby laser pulse or via the singlet manifold with a 3 μsec xenon flash lamp filtered to pass light in the 2500 Å region of the spectrum. The results were the same with either excitation method. The time-decaying x-trap emission signals were detected at right angles with a photomultiplier tube and the monochromator set to the x-trap origin, digitally recorded and signal averaged with a Biomation 805 transient recorder interfaced to a D.G.C. Nova 2 computer. Data was transferred to magnetic tape for subsequent analysis.

Important considerations pertaining to the TCB exciton and trap lifetimes, which spin sublevels are involved in the experiment and the concentration of the TCB x-traps in the samples are dealt with in complete detail in Appendix I. The results of Appendix I are used in the following discussion.

IV. RESULTS

The experiments employed TCB crystals doped with a range of concentrations of the isotopic scattering impurity, d_2-TCB, and the time-dependent phosphorescent emission from the intrinsic TCB x-trap was monitored following impulse optical excitation. Typical data is displayed in Fig. 3. At short times the trap phosphorescence intensity increases as the exciton population flows into the trap. At longer times, all the population has trapped, and the trap emission decays exponentially (see Figure AI-1 Appendix I). As the scattering impurity concentration increases, transport is hindered, the buildup of the trap phosphorescence becomes more gradual, and the maximum is shifted to longer time. In the TCB system it is possible to circumvent difficulties caused by the multiplicity of levels. ESR experiments have demonstrated that spin polarization is preserved on trapping[18] and temperature-dependent measurements have shown that spin-lattice relaxation between triplet sublevels of the first excited state is negligible at liquid He temperatures.[19] Thus, the sublevel populations can be considered to be separate, noninteracting ensembles. In the x-trap, radiative emission from one of the triplet sublevels is symmetry-forbidden to the vibrationless ground state and of the remaining two, another has a negligible radiative rate constant.[20] Thus, x-trap phosphorescence at low temperatures unambiguously reflects the population of a single spin sublevel ensemble (see Appendix I). For the excitons, the symmetry restrictions are lifted and all three sublevels are observed to radiatively decay to the ground state.[19] Using the procedure detailed in Appendix I, it was possible to determine which of the three TCB triplet exciton spin sublevels to associate with the single x-trap triplet spin sublevel under observation. The concentration of x-traps is also obtained in Appendix I. Therefore physical constants which are necessary to use the models described above are known. The trap rate constant for decay to the ground state is $K_T = 25.5\ \text{sec}^{-1}$ and the appropriate exciton decay rate constant in the absence of trapping is $K_E = 35.3\ \text{sec}^{-1}$. The trap concentration is $N_T = 1/22000$. The TCB one-dimensional intermolecular interaction matrix element was previously determined to have a value of $\beta = 0.35\ \text{cm}^{-1}$.[2a,c,d] A reasonable value of the impurity-band center energy difference, S, can be obtained by using the difference between triplet state energies of h_2-TCB and d_2-TCB in a d_2-TCB host crystal. Spectroscopic measurements yield a value of $S = 20.9\ \text{cm}^{-1}$. The concentration of d_2-TCB scattering impurities is known from the sample preparation and all experiments were performed at 1.35 °K.

The functional dependence of the observed time resolved data on scattering impurity concentration is the fundamental test of the importance of exciton-impurity scattering and of the effective exciton trapping topology. As discussed in Sec. II, if the transport topology in TCB is strictly one-dimensional or deviates only slightly from that limit, the observed trapping rate function will vary with scattering impurity concentration in a manner which is directly proportional to $(\chi^{-1} - 1)^{1/2}$, or approximately the inverse square root of the scattering impurity concentration, χ. The concentration dependence of the trapping rate function is determined by the behavior of its time independent coefficients. Using Eq. (7b) and the known decay rate constants, K_E and K_T, an observed trapping rate function coefficient, A, is obtained from the optimal fit to data from each sample. (Equation (18b) could be employed to obtain identical results.) These experimentally determined trapping coefficients are plotted versus $(\chi^{-1} - 1)^{1/2}$ in Fig. 1. The solid line through the data (crosses) shows that the theoretically predicted proportionality occurs over a 30-fold range of concentrations and at all but the lowest scattering impurity concentrations. (The lowest concentration regime is discussed below.) This observation confirms the importance of the role played by scattering impurities in the transport and trapping of triplet excitons in TCB crystals, and demonstrates the applicability of the model to real systems. The deviation from the predicted concentration dependence at low concentrations (doped-in scattering impurities $\leq 0.1\%$) suggests that additional impurities are also present in the samples and that these dominate at low concentrations. This is not an unexpected result since there are, at the very least, additional scattering impurities in the form of the naturally occurring isotopic impurity *hd*-TCB[6] which is 0.03% abundant. Additionally, it is known that trichlorobenzene and tetrachlorobenzene isomers may remain in very low concentration even after extensive zone refining.[13b] Other scattering sites, such as low concentration crystal lattice defects[21] (the high energy counterparts of x-traps), may also hinder transport when the doped-in impurity concentration is sufficiently low to unmask their effects.

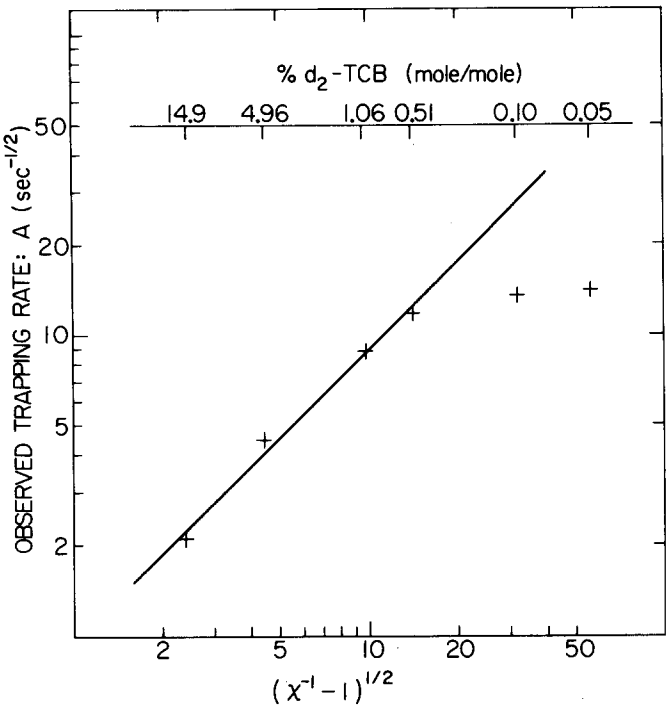

FIG. 1. The experimentally determined trapping rate coefficients, A, of the time-dependent trapping rate function $K_L(t) = At^{-1/2}$ (crosses) are plotted as a function of $(\chi^{-1}-1)^{1/2}$, where χ is the mole fraction of the scattering impurity d_2-TCB doped in various concentrations in h_2-TCB host crystals. The predicted linear dependence, i.e. the solid line, is observed for all but the lowest concentrations. The crosses corresponding to concentrations less than 10^{-3} M/M fall below the line, demonstrating that in this case the d_2-TCB scattering impurities are dominated by residual impurities and intrinsic defects present in the h_2-TCB.

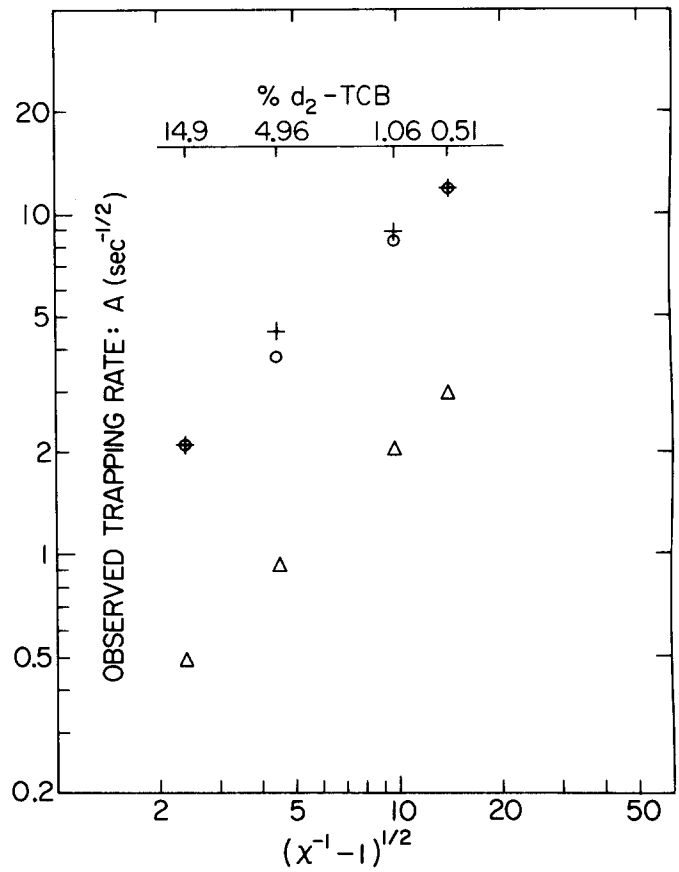

FIG. 2. Theoretically predicted trapping rate constants for TCB in the strictly one-dimensional limit are plotted along with the data (crosses) versus $(\chi^{-1}-1)^{1/2}$, where χ is the mole fraction of scattering impurity. The open circles are calculated for a model of microscopically incoherent exciton migration using the Knox–Kenkre formalism for the site-to-site stepping time. The triangles are calculated for a model of microscopically coherent exciton migration. If small multidimensional interactions are considered, agreement between the data and the coherent model will be greatly improved.

It is clear from the agreement between the experimental and the theoretical scattering impurity concentration dependence that exciton-impurity scattering is the dominant factor in controlling the rate of triplet exciton trapping in TCB. Since all the required physical constants are known for TCB, a realistic upper bound can be placed on the deviation from strict one-dimensionality. First consider the strictly one-dimensional model of Sec. II-A. This model was employed to calculate the trapping rate coefficient, A, without the use of adjustable parameters for both the coherent (Eq. (3)) and incoherent (Eq. (4)) cases. The resulting values of A_{COH} and A_{INCOH} for the various concentrations of the d_2-TCB scattering impurity are given in Table I. These two models predict quite different rates of trapping. The incoherent calculation used Eq. (4b), i.e., the Knox–Kenkre formalism was employed in calculating the microscopic hopping frequency, ν_{INC}. For TCB this approach yields a value of $\nu_{INC} = 1$ psec^{-1} (see Appendix II).

TABLE I. The theoretical trapping rate coefficients, A, for strictly one-dimensional transport in TCB doped with d_2-TCB. A_{COH} is given by Eq. (3). A_{INCOH} is given by Eq. (4) using the theoretically predicted site-to-site hopping time of 1 psec.

% d_2-TCB	A_{COH} (sec$^{-1/2}$)	A_{INCOH} (sec$^{-1/2}$)	
14.9	0.486	2.10	(0.510)[a]
4.96	0.913	3.83	(0.930)
1.06	2.03	8.31	(2.02)
0.51	2.95	11.8	(2.86)

[a]The numbers in parentheses are the results of a calculation which treated the incoherent hopping time as an adjustable parameter, set to 17 psec in Eq. (4a).

The experimental data points and these calculations are plotted in Fig. 2, where it can be seen that the values of A_{INCOH} (circles) agree exceedingly well with the observed data. The coherent transport calculations predict values of A_{COH} (triangles) which are rather too slow to account for the observed results. The actual trapping data and incoherent theoretical curves are displayed in Fig. 3 for each impurity concentration. It can be seen that the overall agreement is excellent. However, the close agreement obtained from the model of incoherent transport may be due to a fortuitous calculation of ν_{INC} using the Knox-Kenkre formula. As discussed in Appendix II, this formula is not exactly

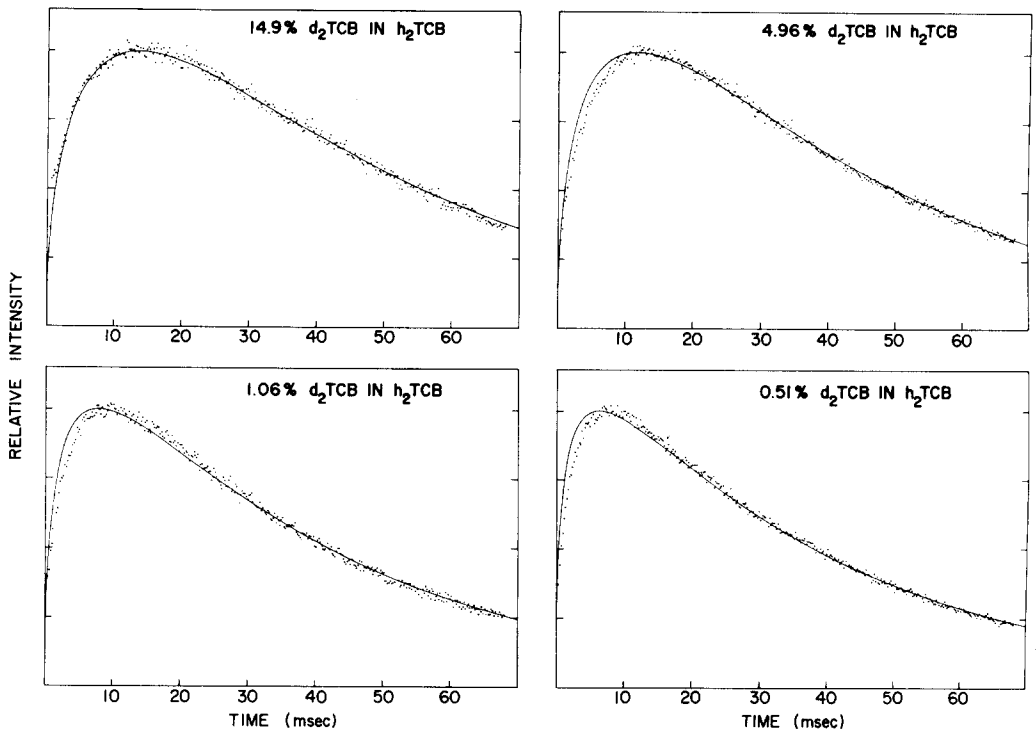

FIG. 3. Time resolved trap emission from TCB crystals doped with various concentrations of scattering impurity. The solid lines are theoretical curves obtained without recourse to adjustable parameters using the model of microscopically incoherent one-dimensional transport and employing the Knox–Kenkre formalism for the incoherent site-to-site stepping frequency.

applicable for the TCB physical situation. If the incoherent site-to-site hopping time is arbitrarily chosen to be $\nu_{INC}^{-1} = 17$ psec, virtually identical results are obtained from the coherent and incoherent models. These results are given in parenthesis in Table I. Furthermore, both calculations neglect the increase in trapping rate which results if interchain interactions do not vanish.

In the TCB system, the $\chi^{-1/2}$ concentration dependence of the trapping shows that any cross chain interaction must be small indeed.[7] If these interactions are not negligible, TCB will behave as a quasi-one-dimensional system and the model of Sec. II-B can be used to interpret the observed time resolved x-trap phosphorescence. The necessary cage-to-cage stepping frequency can be calculated from Eqs. (9) and (10) for coherent and incoherent transport, respectively. The results of these calculations for the various scattering impurity concentrations are given in Table II. Cage stepping frequencies in the linear direction are orders of magnitude slower than the inverse time for site-to-site motion along that direction, typically $\sim 10^{11}$–10^{12} sec^{-1}. Thus, even very low frequency cross chain steps can cause a significant deviation from strictly one-dimensional transport. As discussed in Sec. II-B, the proportionality to $(\chi^{-1} - 1)^{1/2}$ will be observed only if a system is very near the strictly one-dimensional limit, i.e., $\nu_L \gg \nu_C$ and $\nu_{C'}$. If interchain steps were not much slower than intrachain cage-to-cage steps, the transport topology will be much more isotropic and the concentration dependence will be stronger, i.e., it will approach χ^{-1}.[7] Thus, for the TCB the requirement that $\nu_L \gg \nu_C$ implies that interchain steps occur at a rate no greater than $\sim 10^5$ sec^{-1}.

In the absence of an estimate of the anisotropy in the interchain interactions, it is assumed that all such nearest neighbor interactions are equal. In this case the closed form expression describing exciton motion on the three-dimensional superlattice, Eq. (13), may be employed to calculate the trapping rate function, Eq. (8), for each scattering impurity concentration. The different on-chain cage stepping frequencies, ν_L, are given in Table II. Therefore the only unknown parameter is ν_C, and a single choice of ν_C should be able to reproduce the experimental exciton trapping curves for the entire range of scatter impurity concentrations.

Values of ν_C were combined with the values of ν_L(COH) in Table II to evaluate the trapping parameters K_L and B_L via Eq. (11) and Eqs. (13)–(17). These parameters were then used in Eq. (18b) to calculate the time-dependent exciton trapping curves. For coherent transport, the value $\nu_C = 2.5 \times 10^3$ sec^{-1} gave the best overall agreement between theory and the different trapping experiments. The values of K_L and B_L are listed in Table III and the calculated curves along with the experimental data are displayed in Fig. 4. Once again, agreement between observation and theory is generally quite good, although for this model significant disagreement is observed at the greatest impurity concentration. The

TABLE II. The intrachain cage stepping frequency, ν_L, of excitons in TCB doped with d_2-TCB. For coherent transport Eq. (10) was used. For incoherent transport Eq. (11) was employed with a site-to-site hopping time $\nu_{INC}^{-1} = 1$ psec.

% d_2-TCB	ν_L(COH) (sec^{-1})	ν_L (INCOH) (sec^{-1})
14.9	1.02×10^7	9.79×10^7
4.96	3.04×10^6	2.90×10^7
1.06	6.25×10^5	5.76×10^6
0.51	2.99×10^5	2.64×10^6

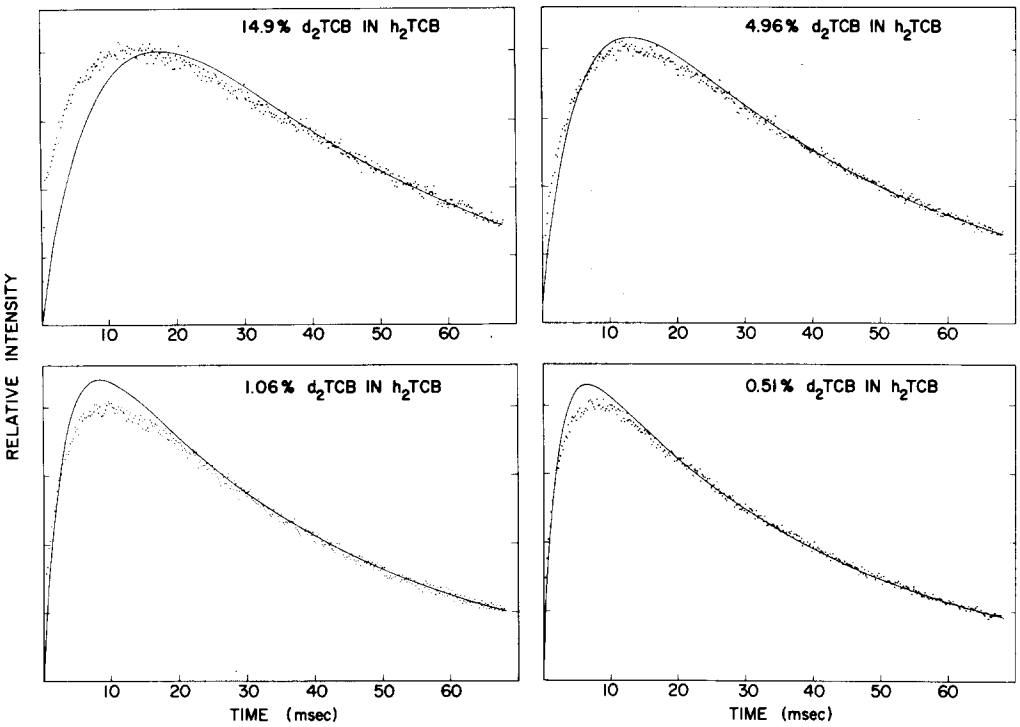

FIG. 4. Time resolved trap emission from TCB crystals doped with various concentrations of scattering impurity and the best fit obtained from the microscopically coherent migration model. In this calculation the extent of multidimensional transport in this basically one-dimensional system was adjusted. The calculated curves were obtained using a cross chain stepping frequency of $\nu_C = 2.5 \times 10^3$ sec^{-1}.

assumption that the cross-chain interactions are isotropic may be partially responsible for the deviations. However, the overall agreement between experiment and both models is sufficiently good that a clear choice between them is not possible. Thus, coherent transport is also consistent with the observed trapping data.

V. DISCUSSION

Observing the effects of scattering impurity concentration on trapping in TCB demonstrates that the TCB triplet exciton system is virtually one-dimensional and that in the samples studied, exciton-impurity scattering is the dominant influence on the macroscopic rate of exciton transport. Furthermore, these results give additional strength to the argument that exciton-impurity scattering strongly influences energy migration in pure TCB crystals as well. From the functional form of the concentration dependence it is possible to put an upper bound on the cross chain stepping frequency of $\sim 10^5$ sec^{-1}. Detailed analysis of the time dependence of the trapping data gives a better estimate of $< 5 \times 10^3$ sec^{-1}. Comparing this to on chain site-to-site transfer frequencies of 10^{11}–10^{12} sec^{-1} shows that the cross chain frequency is down some eight orders of magnitude. Taking the cross chain frequency to be proportional to the square of the cross chain intermolecular interaction would put that interaction at $< 10^{-4}$ of the on chain interaction, corresponding to less than 10^{-4} cm^{-1}. Thus the impurity scattering concentration study provides a sensitive probe of the dimensionality of the exciton transport system.

TABLE III. The theoretical trapping rate coefficients, K_L and B_L, for quasi-one-dimensional transport in TCB doped with d_2-TCB. The intrachain one-dimensional transport is microscopically coherent with cage stepping frequencies given in Table II. The interchain transport is assumed to be isotropic with a cross chain step time $\nu_C = 2.5 \times 10^3$ sec^{-1}.

% d_2-TCB	K_L (sec^{-1})	B_L (sec$^{-1/2}$)
14.9	66.0	0.261
4.96	121	0.478
1.06	267	1.06
0.51	387	1.53

Both the coherent and incoherent microscopic modes are consistant with the experimental trapping data. Impurity scattering forces long range transport to be a diffusive process involving a random walk among cages, irrespective of the microscopic mode of transport. Thus a trapping experiment in this type of system examines the long distance macroscopic rate of transport. Analysis of the trapping data provides the trapping rate parameters once the question of the transport topology has been sorted out. These parameters give directly the cage-to-cage stepping frequency which is the basic quantity characterizing long range energy transport in quasi-one-dimensional systems.

ACKNOWLEDGMENTS

This work was supported by the National Science Foundation, Division of Materials Research grant DMR 76-22019. In addition, acknowledgment is made to the donors of the Petroleum Research Fund, administered

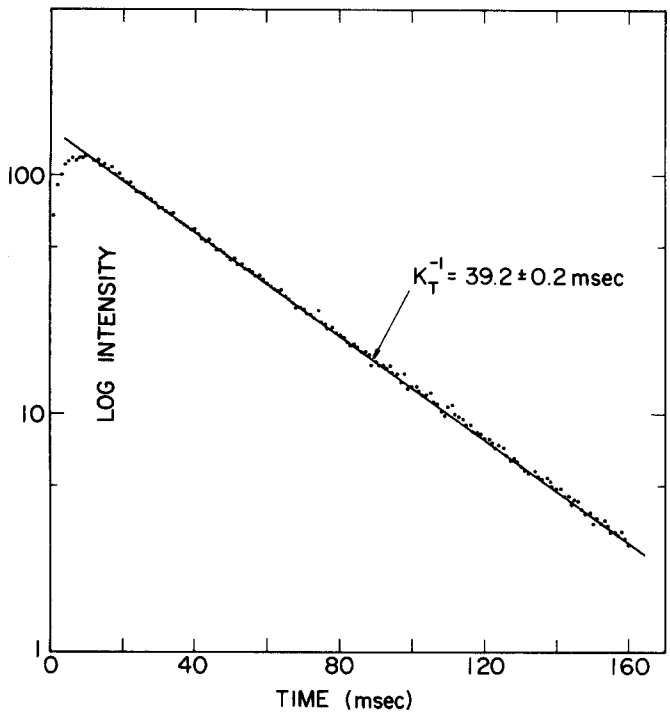

FIG. AI-1. The intensity of time resolved emission from the x-trap of TCB at 1.35 °K following pulsed excitation. The decay is a single exponential with lifetime 39.2 ± 0.2 msec indicating that emission is from a single spin sublevel (see text).

by the American Chemical Society, for partial support of this research.

APPENDIX I

In order to apply the theory presented in this paper to triplet exciton dynamics in TCB it is necessary to accurately determine the physical parameters which allow calculation of the time-dependent trap intensity. These have been obtained by a variety of optical and ESR techniques.

The phosphorescent emission spectrum of pure crystals of TCB at low temperature (1.5–4.2 °K) consists of a vibrational progression of exciton emission originating at 26 676 cm^{-1} and a similar progression of emission originating at 26 658 cm^{-1} due to an x-trap. At 4.2 °K the ratio of exciton emission to x-trap emission at the origin is ~10:1. At 2 °K the same ratio is ~1:10, indicating a transfer of population from band states to trap states.[8a] Several authors have used the temperature dependence of the emission from the x-trap, which is in Boltzmann equilibrium with the band, to determine the excited state intermolecular interaction matrix element, β, and the concentration of x-traps, N_T. Although independent methods have determined β with good agreement,[2a,c,d] values for N_T^{-1} range from 3×10^3 to 2.6×10^5.[2c,8a,13a,b] In this Appendix the various experiments are reinterpreted to show that the data of all authors is consistent with the value $N_T^{-1}=2.2\times10^4$ and that the inconsistencies in the reported values are due either to errors in determining parameters involved in the calculation of N_T or to erroneous assumptions in deriving the relationship between the temperature-dependent trap intensity and N_T.

This relationship is obtained from the partition function for the exciton band-trap system, $Z(T)$.[2c] For any number of band states ≥ 20, $Z(T)$ rapidly converges to

$$Z(T)=1+e^{(2\beta-\Delta)/KT}I_0(y)/N_T\,, \qquad \text{(AI-1)}$$

where Δ is the trap depth, i.e., the spectroscopically observable splitting between $k=0$ and the trap state, K is Boltzmann's constant, and the zero of energy is at the trap. $I_0(y)$ is the zeroth order modified Bessel function of argument y, where $y=|2\beta/KT|$. For TCB in the range $2\,°K\leq T\leq 5\,°K$, $1.01\leq I_0(y)\leq 1.05$, so that this term could be set to unity. The fraction of population in the trap is given by $\chi(T)=Z(T)^{-1}$. However, in the case that the exciton and trap lifetimes are unequal, the temperature-dependent partitioning of excitation between the states results in a temperature dependent total ensemble population.[2c,8a] In this case the observed intensity is the product of the trap sublevel radiative rate constant, the total population, and $\chi(T)$. In Ref. 2c this is given by

$$I(T)=I(T_r)\left[\frac{K_T\chi(T_r)+K_E(1-\chi(T_r))}{K_T\chi(T)+K_E(1-\chi(T))}\right]\frac{\chi(T_r)}{\chi(T)}\,, \qquad \text{(AI-2)}$$

where T_r is a reference temperature. All intensities are scaled with respect to $I(T_r)$, the intensity at this reference temperature. This procedure eliminates the trap radiative rate constant. Treating all terms which depend on T_r as constants, the resulting trap intensity (as suggested by Knox[22]) is

$$I(T)=C\left[1+\frac{K_E}{K_TN_T}I_0(y)\,e^{(2\beta-\Delta)/KT}\right]^{-1}\,. \qquad \text{(AI-3)}$$

Thus N_T can be determined as accurately as β, Δ, K_E, and K_T. Figure AI-1 is a log plot of phosphorescence intensity of the x-trap origin of TCB versus time at 1.5 °K following impulse excitation. After the trap buildup, the decay is a single exponential with lifetime 39.2 ± 0.2 msec, i.e., $K_T=25.5\ sec^{-1}$. (This corresponds to a single trap sublevel as discussed in Sec. IV.) ESR experiments indicate that spin polarization is preserved upon trapping[18] and a detailed analysis of the exciton decay from steady state as a function of temperature in the range 4.2–80 °K demonstrates that the effect of spin-lattice relaxation (SLR) is minor at 4.2 °K.[19] Therefore, only one spin sublevel exciton band communicates with the single trap sublevel which is observed in this experiment.

The time-dependent emission from the exciton band origin at 4.2 °K was obtained and clearly decomposable into three exponentially decaying components with lifetimes of 2.7, 11, and 28.4 msec.[19] At 4.2 °K trapping is negligible and the data is taken to be emission from the three independent triplet spin sublevel bands. Since SLR at this temperature is very slow, the observed decay rates are very close to the actual decay rates. At temperatures below 4.2 °K the decay is dominated by trapping and therefore it is difficult to obtain accurate lifetime information.

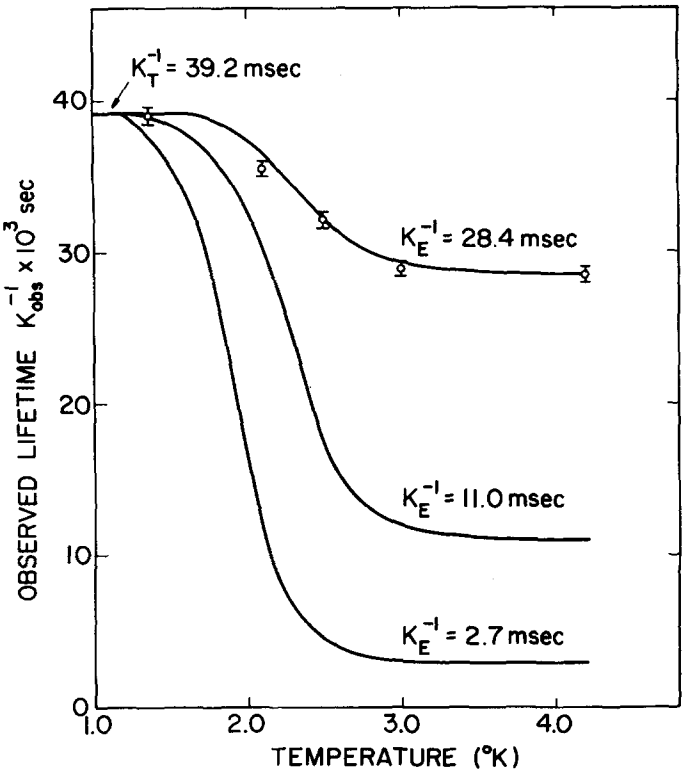

FIG. AI-2. Results of a temperature dependent study of the observed decay rate for time resolved trap emission from h_2-TCB (soild circles). The observed trap decay rate will be an average of the band and trap rate constants weighted by the appropriate Boltzmann factors. The individual band sublevels in TCB have lifetimes of 28.4 msec, 11.0 and 2.7 msec. The solid curves are the theoretical predictions for coupling between the observed trap sublevel (see Fig. AI-1) and the possible band sublevels. The temperature dependence demonstrates that the trap sublevel is coupled to the 28.4 msec exciton band sublevel.

In order to determine whether the fast (2.7 msec), medium (11 msec), or slow (28 msec) exciton sublevel is involved in the trapping experiments, the temperature dependence of the apparent trap lifetime was studied. In the region between 1.8 and 4.2 °K the existence of thermal equilibrium implies fast exchange of population between band and trap. Thus the observed trap decay constant should approach the band rate constant as the temperature increases. Figure AI-2 plots the observed lifetime of the single trap sublevel which emits to the origin versus temperature. The solid lines in Fig. AI-2 are calculated curves assuming rapid equilibration between the trap and band for the fast, medium, and slow band sublevels. These curves are calculated using the relation

$$K_{obs} = \chi(T)K_T + (1-\chi(T))K_E\,, \qquad \text{(AI-4)}$$

that is, a weighted average of the trap and band decay rates. From Fig. AI-2 it is clear that the apparent rate constant can only be due to population exchange between the single trap sublevel observed in the trapping experiments and the slow (28.4 msec) exciton sublevel. Thus, we can assign $K_E = 35.3\ \text{sec}^{-1}$. In the determination of N_T the greatest error is in K_E since SLR may not be completely absent at 4.2 °K. However, this value is accurate within 10% and from Eq. (AI-3) this will result in an uncertainty of 10% in N_T.

The value for Δ is $17.3 \pm 0.2\ \text{cm}^{-1}$. This has been determined by several groups and by two independent means: by emission spectroscopy[2c] and by a determination of the activation energy for detrapping.[13b] In Ref. 2a and 22 the erroneous value $\Delta = 21.3\ \text{cm}^{-1}$ appeared and this value was used by several subsequent authors.[8a,13a] All workers now agree that the $17.3\ \text{cm}^{-1}$ value is indeed correct.

This leaves β and N_T as the only unknown parameters which determine the nature of the temperature-dependent trap intensity. In Ref. 2c the data are in excellent agreement with theory for $\beta = 0.34\ \text{cm}^{-1}$ and $N_T^{-1} = 5500$. However, in this work K_E is given as $150\ \text{sec}^{-1}$. This erroneous rate constant was obtained from a single exponential fit to a multiexponential decay. Since Eq. (AI-3) contains only the ratio K_E/N_T, an error in K_E will produce the same error in N_T. Thus the correct exciton rate constant results in the values, $\beta = 0.34\ \text{cm}^{-1}$ and $N_T^{-1} = 2.2 \pm 0.2 \times 10^4$. The revised calculated intensity is unchanged and appears exactly as in Ref. 2c. An interesting feature of this data is that the value of $4\beta = 1.35\ \text{cm}^{-1}$ determined by trap intensity agrees very closely with the value $4\beta = 1.25\ \text{cm}^{-1}$ determined by optical detection of the exciton band-to-band ESR transition by workers in the United States in 1971,[2a] and the value $4\beta = 1.40\ \text{cm}^{-1}$ determined by conventional ESR methods in the Netherlands in 1977.[2d] It should be noted that the value of $4\beta = 0.6$ which was reported in Ref. 23 and employed in Ref. 13b, was "estimated" from the intensity of ESR transitions between TCB dimers in d_2-TCB host. Although this estimate is in fair agreement with the *measured* values, it is by no means as accurate a determination as those discussed in the above three references.

Finally, we turn our attention to the wide discrepancy between literature values of N_T. Fayer and Harris[8a] developed the theory of band-trap equilibrium and made the first determination by this method of $4\beta = 3.5\ \text{cm}^{-1}$ and $N_T^{-1} = 9 \times 10^4$, but incorrectly took $\Delta = 21.3\ \text{cm}^{-1}$. We have reanalyzed the data in this work and find that with the correct trap depth it gives within experimental error the correct values for β and N_T. In Ref. 13a the temperature dependent method was again used to determine a value of $N_T^{-1} = 2.56 \times 10^5$. Here, once again, the incorrect trap depth was used which results in a sizable overestimation of N_T^{-1}.

The most recent determination of $N_T^{-1} = 3 \pm 1 \times 10^3$ by Wolf *et al.*,[13b] although experimentally accurate is flawed by an incorrect analysis of the relationship between N_T and the observed intensity of steady state trap and band emission. Equation (9) of that work gives (in our notation)

$$\left(\frac{P_T}{P_E}\right)_{ST} = N_T \exp(\Delta/KT) \qquad \text{(AI-5)}$$

where $(P_T/P_E)_{ST}$ is the ratio of the trap and band populations in steady state at temperature T. By comparison with Eq. (AI-3) it can be seen that the assumptions im-

plicit in Eq. (AI-6) are: 1) the bandwidth $4\beta = 0$, and 2) the ratio $K_E/K_T = 1$. For the TCB system, these assumptions are fairly accurate since the finite bandwidth contributes only a few percent error and we have determined $K_E/K_T \approx 1.4$, a 40% error. However, the flaw in this determination is the assumption that the observed ratios of trap and band *intensities* are equal to the ratios of the trap and band sublevel *populations* i.e., $(I_T/I_E)_{ST} = (P_T/P_E)_{ST}$. The radiative rate constants for decay to the exciton and trap origins are assumed identical. This in general is not realistic. The correct form of Wolf's equation should be

$$\left(\frac{I_T}{I_E} \cdot \frac{K_E^r}{K_T^r}\right)_{ST} = \left(\frac{P_T}{P_E}\right)_{ST} = N_T \exp(\Delta/KT), \qquad \text{(AI-6)}$$

where K_T^r and K_E^r are the radiative rate constants for the observed sublevels. The fact that these radiative rate constants are not identical can be seen from the data of every worker in this field. For example Fig. 2 from Wolf *et al.*[13b] shows the temperature dependence of phosphorescence intensity of band origin and trap origin emission. At 4.2 °K the relative intensities are band ≈8 and trap ≈0.7, and at 2.5 °K they are band ≈6, trap ≈35. Transfer of population from band to trap would result in a constant total emission intensity if the radiative rate constants are identical. This clearly is not the case in the TCB system, and in fact the above data are more consistent with $K_T^r \gg K_E^r$. This results in a substantial underestimation of N_T^{-1} using Eq. (AI-5). Furthermore, the fact that exciton emission occurs from all three triplet spin sublevels in the band but from only one trap sublevel is ignored. The way to approach the data is to use Eq. (AI-3) and compare the intensity of trap emission at one temperature to the trap intensity at another temperature since the radiative rate constant divides out of the equation in the case of the TCB-x-trap where only a single sublevel is observed.

APPENDIX II

If exciton transport is dominated by fast stochastic exciton–phonon scattering, then exciton motion is incoherent and may be described by a site-to-site stepping frequency ν_{INC}. Knox and Kenkre have constructed a formalism which employs an exponentially decaying coherence memory function to describe the loss of exciton coherence through phonon interactions.[3a] If the rate of coherence loss, α, is large relative to β/h, the "rate of energy transfer," i.e., $\alpha \gg \beta/h$, then transport occurs according to the "slow transfer" rate, Eq. (5) of Sec. II. The exponential form of the coherence memory function implies that the exciton band optical absoption lineshape will be Lorentzian of half-width α.

High resolution optical absorption measurements have been made on the exciton band origin of TCB at low temperatures.[4a] These experiments showed that the absorption line at liquid He temperatures is Lorentzian with half-width 0.59 cm^{-1}. The decay rate $\alpha = 0.59$ $cm^{-1}/h = 1.8 \times 10^{10}$ sec^{-1}. In contrast, the "rate of transfer" $\beta/h = 1.0 \times 10^{10}$ sec^{-1}. At liquid He temperatures, TCB is not a clearcut case for "slow transfer" since the requirement $\alpha \gg \beta/h$ is only approximately met. Thus, the calculation of the incoherent site-to-site stepping frequency should be taken as an estimate. The result is $\nu_{INC} = 9.9 \times 10^{11}$ sec^{-1}, or a step time of 1 psec.

[1] J. Frenkel, Phys. Rev. 37, 17 (1931); 37, 1276 (1931); A. S. Davydov, *Theory of Molecular Excitons* (Plenum, New York, 1971); *Abstracts of the Eighth Molecular Crystal Symposium* (Santa Barbara, California, 1977).

[2] (a) A. H. Francis and C. B. Harris, Chem. Phys. Lett. 9, 181, 188 (1971); (b) R. M. Hochstrasser and J. D. Whiteman, J. Chem. Phys. 56, 5945 (1972); (c) D. D. Dlott and M. D. Fayer, Chem. Phys. Lett. 41, 305 (1976); (d) B. J. Botter, A. I. M. Dicker, and J. J. Schmidt (in press).

[3] (a) V. M. Kenkre and R. S. Knox, Phys. Rev. B 9, 5279 (1974); Phys. Rev. Lett. 33, 804 (1974); (b) M. Grover and R. Silbey, J. Chem. Phys. 52, 2099 (1970).

[4] (a) D. M. Burland, D. E. Cooper, M. D. Fayer, and C. R. Gochanour, Chem. Phys. Lett. 52, 279 (1977); (b) D. M. Burland, U. Konzelmann, and R. M. Macfarlane, J. Chem. Phys. 67, 1926 (1977).

[5] (a) R. Kopelman, "Radiationless Processes in Molecules and Condensed Phases," in *Topics in Applied Physics*, edited by Francis K. Fong (Springer, New York, 1976), Vol. 15; (b) J. Hoshen and R. Kopelman, J. Chem. Phys. 65, 2817 (1976); J. Klafter and J. Jortner, Chem. Phys. Lett. 49, 410 (1977); 50, 202 (1977); J. Chem. Phys. 68, 1513 (1978).

[6] D. D. Dlott, M. D. Fayer, and R. D. Wieting, J. Chem. Phys. 67, 3803 (1977).

[7] R. D. Wieting, M. D. Fayer, and D. D. Dlott, J. Chem. Phys. 69, 1996 (1978).

[8] (a) M. D. Fayer and C. B. Harris, Phys. Rev. B 9, 748 (1974); (b) M. D. Fayer and C. R. Gochanour, J. Chem. Phys. 65, 2472 (1976).

[9] R. M. Pearlstein, J. Chem. Phys. 56, 2431 (1972); R. P. Hemenger, R. M. Pearlstein, and K. Lakatos-Lindenberg, J. Math. Phys. 13, 1057 (1972); R. P. Hemenger and R. M. Pearlstein, Chem. Phys. 2, 424 (1973); R. P. Hemenger, K. Lakatos-Lindenberg, and R. M. Pearsltein, J. Chem. Phys. 60, 3271 (1974).

[10] H. Sumi and Y. Toyozawa, J. Phys. Soc. Jpn. 31, 342 (1971); C. B. Harris, J. Chem. Phys. 67, 5607 (1977).

[11] M. D. Fayer and C. B. Harris, Chem. Phys. Lett. 25, 149 (1974); H. C. Brenner, J. C. Brock, M. D. Fayer, and C. B. Harris, Chem. Phys. Lett. 33, 471 (1975).

[12] R. C. Powell and Z. G. Soos, J. Lumin, 11, 1 (1975).

[13] (a) R. M. Shelby, A. H. Zewail, and C. B. Harris, J. Chem. Phys. 64, 3192 (1976); (b) W. Guettler, J. O. von Schuetz, and H. C. Wolf, Chem. Phys. 24, 159 (1977).

[14] G. F. Koster and J. C. Slater, Phys. Rev. 95, 1167 (1954); 96, 1208 (1954).

[15] E. W. Montroll, Proc. Symp. Appl. Math. Am. Math. Soc. 16, 193 (1964).

[16] D. A. Zwemer and C. B. Harris, J. Chem. Phys. 68, 2184 (1978).

[17] E. W. Montroll, *Proceedings of the* 3rd *Berkeley Symposium on Mathematical Statistics and Probability* (University of California, Berkeley, 1956), Vol. III, p. 209.

[18] A. H. Francis and C. B. Harris, J. Chem. Phys. 55, 3595 (1971).

[19] M. D. Fayer, D. R. Lutz, K. A. Nelson, and R. W. Olsen, J. Chem. Phys. (to be published).

[20] A. H. Francis and C. B. Harris, J. Chem. Phys. 57, 1050 (1972).

[21] R. H. Baughman and D. Turnbull, J. Phys. Chem. Solids 32, 1375 (1971).

[22] R. S. Knox and M. A. Davidovich (private communication).

[23] A. H. Zewail and C. B. Harris, Chem. Phys. Lett. 28, 8 (1974).